Measurement of single π^0 production in neutral current neutrino interactions with water by a 1.3 GeV wide band muon neutrino beam

S.Nakayama [a], C.Mauger [b,1], M.H.Ahn [c], S.Aoki [d], Y.Ashie [a], H.Bhang [c], S.Boyd [e,1], D.Casper [f], J.H.Choi [g], S.Fukuda [a], Y.Fukuda [h], R.Gran [e], T.Hara [d], M.Hasegawa [i], T.Hasegawa [j], K.Hayashi [i], Y.Hayato [k], J.Hill [b,1], A.K.Ichikawa [k], A.Ikeda [ℓ], T.Inagaki [i,1], T.Ishida [k], T.Ishii [k], M.Ishitsuka [a], Y.Itow [a], T.Iwashita [k], H.I.Jang [g,1], J.S.Jang [g], E.J.Jeon [c], K.K.Joo [c], C.K.Jung [b], T.Kajita [a], J.Kameda [a], K.Kaneyuki [a], I.Kato [i,1], E.Kearns [m], A.Kibayashi [n], D.Kielczewska [o,p], B.J.Kim [c], C.O.Kim [q], J.Y.Kim [g], S.B.Kim [c], K.Kobayashi [b], T.Kobayashi [k], Y.Koshio [a], W.R.Kropp [f], J.G.Learned [n], S.H.Lim [g], I.T.Lim [g], H.Maesaka [i], T.Maruyama [k,1], S.Matsuno [n], C.Mcgrew [b], A.Minamino [a], S.Mine [f], M.Miura [a], K.Miyano [r], T.Morita [i], S.Moriyama [a], M.Nakahata [a], K.Nakamura [k], I.Nakano [ℓ], F.Nakata [d], T.Nakaya [i], T.Namba [a], R.Nambu [a], K.Nishikawa [i], S.Nishiyama [d], K.Nitta [k], S.Noda [d], Y.Obayashi [a], A.Okada [a], Y.Oyama [k], M.Y.Pac [s], H.Park [k,1], C.Saji [a], M.Sakuda [k,1], A.Sarrat [b], T.Sasaki [i], N.Sasao [i], K.Scholberg [u,t], M.Sekiguchi [d], E.Sharkey [b], M.Shiozawa [a], K.K.Shiraishi [e], M.Smy [f], H.W.Sobel [f], J.L.Stone [m], Y.Suga [d], L.R.Sulak [m], A.Suzuki [d], Y.Suzuki [a], Y.Takeuchi [a], N.Tamura [r], M.Tanaka [k], Y.Totsuka [k], S.Ueda [i], M.R.Vagins [f], C.W.Walter [u], W.Wang [m], R.J.Wilkes [e], S.Yamada [a,1], S.Yamamoto [i], C.Yanagisawa [b], H.Yokoyama [v], J.Yoo [c], M.Yoshida [w], J.Zalipska [p]

[a] *Institute for Cosmic Ray Research, University of Tokyo, Kashiwa, Chiba 277-8582, JAPAN*

[b] *Department of Physics and Astronomy, State University of New York, Stony Brook, NY 11794-3800, USA*

[c] *Department of Physics, Seoul National University, Seoul 151-742, KOREA*

[d] *Kobe University, Kobe, Hyogo 657-8501, JAPAN*

[e] *Department of Physics, University of Washington, Seattle, WA 98195-1560, USA*

[f]*Department of Physics and Astronomy, University of California, Irvine, Irvine, CA 92697-4575, USA*

[g]*Department of Physics, Chonnam National University, Kwangju 500-757, KOREA*

[h]*Department of Physics, Miyagi University of Education, Sendai 980-0845, JAPAN*

[i]*Department of Physics, Kyoto University, Kyoto 606-8502, JAPAN*

[j]*Research Center for Neutrino Science, Tohoku University, Sendai, Miyagi 980-8578, JAPAN*

[k]*High Energy Accelerator Research Organization (KEK), Tsukuba, Ibaraki 305-0801, JAPAN*

[ℓ]*Department of Physics, Okayama University, Okayama, Okayama 700-8530, JAPAN*

[m]*Department of Physics, Boston University, Boston, MA 02215, USA*

[n]*Department of Physics and Astronomy, University of Hawaii, Honolulu, HI 96822, USA*

[o]*Institute of Experimental Physics, Warsaw University, 00-681 Warsaw, POLAND*

[p]*A. Soltan Institute for Nuclear Studies, 00-681 Warsaw, POLAND*

[q]*Department of Physics, Korea University, Seoul 136-701, KOREA*

[r]*Department of Physics, Niigata University, Niigata, Niigata 950-2181, JAPAN*

[s]*Department of Physics, Dongshin University, Naju 520-714, KOREA*

[t]*Department of Physics, Massachusetts Institute of Technology, Cambridge, MA 02139, USA*

[u]*Department of Physics, Duke University, Durham, NC 27708, USA*

[v]*Department of Physics, Tokyo University of Science, Noda, Chiba 278-0022, JAPAN*

[w]*Department of Physics, Osaka University, Toyonaka, Osaka 560-0043, JAPAN*

The K2K Collaboration

Abstract

Neutral current single π^0 production induced by neutrinos with a mean energy of 1.3 GeV is measured using a 1000 ton water Cherenkov detector in the K2K long baseline neutrino experiment. The cross section for this process relative to the total charged current cross section is measured to be $0.064 \pm 0.001\,(stat.) \pm 0.007\,(sys.)$. The momentum distribution of neutral current π^0s from a water target is measured with high statistics for the first time.

Key words:
PACS: 13.15.+g, 14.60.Lm, 25.30.Pt

After the discovery of atmospheric neutrino oscillations by Super-Kamiokande in

[1] For current affiliations see `http://neutrino.kek.jp/address05may.pdf` .

1998 [1], the primary aim of current and future long baseline (LBL) experiments using an accelerator-based neutrino beam is the accurate determination of oscillation parameters. The uncertainties on the knowledge of the neutrino-nucleus cross sections and subsequent nuclear effects in the GeV neutrino energy region could become a severe limitation in future oscillation studies. Near detectors of LBL experiments can provide neutrino interaction data with much higher statistics and better quality to reduce these systematic uncertainties.

Single π^0 events are a good signature of neutral current (NC) neutrino interactions in the GeV region, and in a water Cherenkov detector a decay of the π^0 can be clearly identified as two electromagnetic-showering Cherenkov rings. Understanding this rate will make several significant contributions. The single π^0 production rate by atmospheric neutrinos could be used to distinguish between the $\nu_\mu \leftrightarrow \nu_\tau$ and $\nu_\mu \leftrightarrow \nu_s$ oscillation hypotheses. The NC rate is attenuated in the case of transitions of ν_μ's into sterile neutrinos, while it does not change in the $\nu_\mu \leftrightarrow \nu_\tau$ scenario. In addition, understanding single π^0 production is important for electron neutrino appearance searches at LBL experiments using a water Cherenkov far detector. In these experiments, the most serious background comes from events with a single π^0 where only one ring is found due to highly asymmetric energies, or a small opening angle between the γ-rays of the decay [2]. These single π^0s in the GeV neutrino energy region are mainly produced via the Δ resonance as $\nu + N \rightarrow \nu + \Delta,\ \Delta \rightarrow N' + \pi^0$, where N and N' are nucleons. Because of nuclear effects such as Fermi motion, Pauli blocking, nuclear potential and final state interactions, Δ production and its decay could be different from a simple picture of neutrino-nucleon interactions. In addition, final state interactions of nucleons and mesons during propagation inside of nuclear matter could substantially modify the number, momenta, directions and charge states of produced particles. Though there are several theoretical approaches for modeling these processes, their uncertainties are large and there exist very few experimental data for NC single π^0 production with no measurements using a water target, the target material used in the far detector of some LBL experiments [3,4]. It is clear that good knowledge of the NC single π^0 production cross section and π^0 momentum distribution is required for the above studies. In this letter, we present the first high statistics measurement of "NC1π^0 interactions in water" defined as a neutral current neutrino interaction where a single π^0 and no other mesons are emitted in the final state from the target nucleus.

The KEK to Kamioka long baseline neutrino oscillation experiment (K2K) uses an almost pure muon neutrino beam (98.2 % ν_μ, 1.3 % ν_e and 0.5 % $\overline{\nu}_\mu$) with a mean neutrino energy of 1.3 GeV. This intense wide-band beam is produced by the KEK proton synchrotron (KEK-PS). Protons extracted from the KEK-PS with 12 GeV kinetic energy are bent toward the far detector, Super-Kamiokande, located 250 km away from KEK and interact with an aluminum target. Positively charged

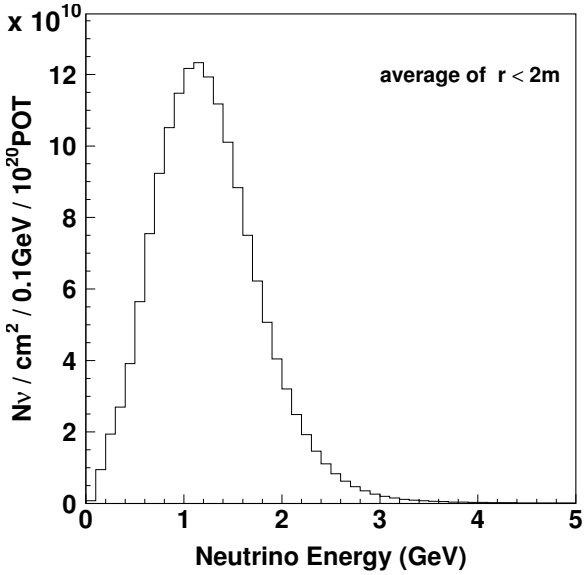

Fig. 1. The energy spectrum of the K2K neutrino beam at 300 m downstream from the target with a 10^{20} protons on target exposure as predicted by a neutrino beam simulation. The spectrum is averaged within 2 m from the beam center.

secondary particles, mainly π^+'s, are focused with a pair of magnetic horns and then decay to produce a neutrino beam. Figure 1 shows the energy spectrum of the K2K neutrino beam at 300 m downstream from the target with a 10^{20} protons on target (p.o.t.) exposure as predicted by a beam simulation [3]. The beam simulation is validated by a pion monitor, which measures the momentum and divergence of pions just behind the second horn [3]. The flux shape is also measured through neutrino interactions by the K2K near detectors [5]. The absolute neutrino flux is not estimated for the measurement of the NC1π^0 cross section because it is difficult to verify the proton beam intensity, profile and targeting efficiency uncertainties. Instead of deriving the absolute cross section, we measure the relative cross section of NC1π^0 interactions to the total charged current (CC) cross section.

As one of the near detectors for K2K, a 1,000 ton water Cherenkov detector (1kt) is located about 300 m downstream of the pion production target. The 1kt detector is a miniature of Super-Kamiokande using the same interaction target material and instrumentation. The inner volume of the 1kt detector is a cylinder of 8.6 m in diameter and 8.6 m in height. This volume is viewed by 680 photomultiplier tubes (PMTs) of 50 cm diameter, facing inward to detect Cherenkov light from neutrino events. The PMTs and their arrangement are identical to those of Super-Kamiokande, giving a 40 % photocathode coverage. The primary role of the 1kt detector is to measure the ν_μ interaction rate and the ν_μ energy spectrum. The 1kt detector also provides a high statistics measurement of neutrino-water interactions. The analysis in this letter is based on 1kt data taken between January 2000 and July 2001, corresponding to 3.2×10^{19} p.o.t. .

The 1kt detector data acquisition (DAQ) system is also similar to that of Super-

Kamiokande. The signal from each PMT is processed using custom electronics modules called ATMs, which were developed for the Super-Kamiokande experiment and are used to record digitized charge and timing information for each PMT hit over a threshold of about $1/4$ photoelectron [6]. The DAQ trigger threshold is about 40 PMT hits within a 200 nsec time window in a 1.2 μsec beam spill gate. This is roughly equivalent to the signal of a 6 MeV electron. The analog sum of all 680 PMTs' signals (PMTSUM) is also recorded for every beam spill by a 500 MHz FADC to identify multiple interactions in a spill gate. We determine the number of interactions in each spill by counting the peaks in PMTSUM greater than a threshold equivalent to a 100 MeV electron signal.

The physical parameters of an event in the 1kt detector such as the vertex position, the number of Cherenkov rings, particle types and momenta are determined by using the same algorithms as in Super-Kamiokande [7,8]. First, the vertex position of an event is determined from the PMT timing information. With knowledge of the vertex position, the number of Cherenkov rings and their directions are determined by a maximum-likelihood procedure. Each ring is then classified as *e*-like, representing a showering particle ($e^{\pm}$, γ), or μ-like, representing a non-showering particle ($\mu^{\pm}$, $\pi^{\pm}$), using its ring pattern. On the basis of this particle type information, the vertex position of a single-ring event is further refined. The momentum corresponding to each ring is determined from the Cherenkov light intensity.

In the 1kt detector, the gain and timing of each PMT are calibrated using a Xe lamp and a N_2 laser as light sources, respectively. The absorption and scattering coefficients of water are measured by a laser calibration, and the coefficients in the detector simulation are further tuned to reproduce the observed charge patterns of cosmic ray muon events. The number of photoelectrons per unit track length is calibrated by cosmic ray muons passing through the detector. The energy scale is checked by cosmic ray muons stopping inside the detector for which the track length is determined by the vertex position of subsequent decay electron events. The accuracy of the energy scale is estimated to be $^{+2}_{-3}$ %. The performance of vertex reconstruction is experimentally studied by special cosmic ray muon data utilizing a pipe inserted vertically into the tank. Cosmic ray muons going through the pipe emulate the neutrino-induced muons whose vertex position is defined at the bottom end of the pipe. This study demonstrates the vertex reconstruction works as we expected from the Monte Carlo simulation.

Neutrino interaction candidates are selected by the following requirements : (i) An event is triggered within a 1.2 μsec beam spill gate. (ii) There is no detector activity within a 1.2 μsec window preceding the beam spill. (iii) Only a single event is found by the PMTSUM peak search in that spill. (iv) The vertex is reconstructed in the 25 ton fiducial volume defined as a 4 m diameter and 2 m long cylinder along the beam axis. (v) The visible energy is larger than 30 MeV. A total of 60,545 events

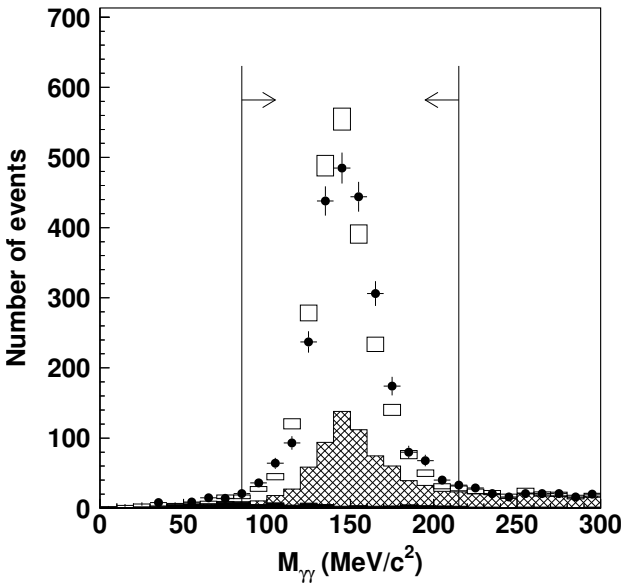

Fig. 2. The invariant mass of two *e*-like ring events for the experimental data (black dots) and the neutrino Monte Carlo simulation (box histogram). The Monte Carlo histogram is normalized to the area of the data histogram. The error bars are statistical only. The hatched portion and the black portion in the Monte Carlo histogram show the non-NC1π^0 component and the non-π^0 component, respectively. A pair of arrows shows the invariant mass cut (3) (see text).

are selected by requirements (i) to (v).

Single π^0 events are extracted from the sample of fully contained (FC) neutrino events, which deposit all of their Cherenkov light inside the inner detector. An exiting particle deposits a large amount of energy at the PMT of the exiting position. Therefore, the FC events are selected by requiring the maximum number of photoelectrons on a single PMT at the exit direction of the most energetic particle to be less than 200. The events with the maximum number of photoelectrons greater than 200 are identified as a partially contained (PC) event. Because π^0s mostly decay into two γ-rays, the following cut criteria are further applied to select the single π^0 events in the FC sample : (1) The number of reconstructed rings is two. (2) Both rings have a showering type (*e*-like) particle identification. (3) The invariant mass is in the range of $85-215\,\mathrm{MeV}/c^2$. Figure 2 shows the invariant mass distribution of the events which satisfy cuts (1) and (2). A π^0 mass peak is clearly observed. The peaks for both the observed data and the neutrino Monte Carlo events are slightly shifted towards higher values compared to the nominal value of the π^0 mass, $135\,\mathrm{MeV}/c^2$. This shift is due to $\sim$20 cm bias of vertex reconstruction for γ-rays from π^0 decay and energy deposited by de-excitation γ-rays from the oxygen nucleus. The difference in peak position between the data distribution and the Monte Carlo prediction is within our quoted $^{+2}_{-3}$ % systematic uncertainty for the absolute energy scale. As shown in Table 1, a total of 2,496 events are found as the single π^0 sample by these criteria.

	Data	NC1π^0 efficiency
FC	45317	97 %
Two rings	11117	57 %
Both *e*-like	3150	48 %
Invariant mass	2496	47 %

Table 1
The number of events after each selection to make the single π^0 sample in 1kt data. The Monte Carlo efficiencies are calculated for NC1π^0 interactions whose real vertex is in the fiducial volume.

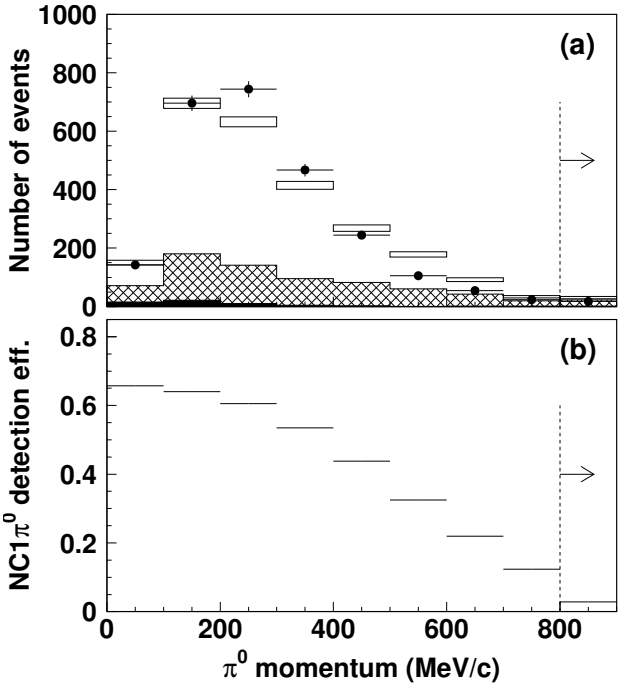

Fig. 3. (a) The reconstructed π^0 momentum distribution for the single π^0 sample, comparing 1kt data (black dots) and the neutrino Monte Carlo simulation (box histogram). The Monte Carlo histogram is normalized to the area of the data histogram. The error bars are statistical only. The hatched portion and the black portion in the Monte Carlo histogram show the non-NC1π^0 component and the non-π^0 component, respectively. (b) The detection efficiency for NC1π^0 interactions as a function of real π^0 momentum. The highest momentum bin in each figure integrates the events above 800 MeV/*c*.

Figure 3 -(a) shows the reconstructed π^0 momentum distribution for the single π^0 sample. The momentum resolution is estimated to be 15 MeV/*c* for π^0s with a momentum of 200 MeV/*c*. As shown by the hatched portion and the black portion in Figures 2 and 3 -(a), the single π^0 sample containes the non-NC1π^0 component and the non-π^0 component, which are both the backgrounds to our signal, NC1π^0 interactions. The non-NC1π^0 component consists of events which include π^0s but do not satisfy our definition of NC1π^0 interactions. The composition of the non-NC1π^0 component is described later. The non-π^0 component consists of back-

ground events with no π^0. As described in detail later, the fraction of each component is estimated by the neutrino Monte Carlo simulation and the background components are subtracted from the single π^0 sample.

The neutrino interactions with water are simulated by the NEUT program library. A detailed description of NEUT can be found in Ref. [9]. Quasi-elastic scattering is simulated based on the Llewellyn Smith's model [10]. The Rein and Sehgal model [11] is used to simulate single meson production mediated by a baryon resonance. The decay kinematics of the $\Delta(1232)$ resonance is also determined by the Rein and Sehgal method. For the decays of the other resonances, the generated mesons are assumed to be emitted isotropically in the resonance rest frame. A 20 % suppression of pion production is adopted for simulating pion-less Δ decay, where the event contains only a lepton and a nucleon in the final state [12]. The axial vector mass, M_A, is set to $1.1\,\mathrm{GeV}/c^2$ for both the quasi-elastic scattering and the single meson production models. Coherent pion production is simulated using the Rein and Sehgal model [13] with modified cross section according to a description by Marteau et al. [14]. For deep inelastic scattering, GRV94 nucleon structure function [15] with a correction by Bodek and Yang [16] is used to calculate the cross section. In order to generate the final state hadrons, the PYTHIA/JETSET [17] package is used for hadronic invariant masses W larger than $2.0\,\mathrm{GeV}/c^2$. A custom program [18] is used for W in the range of $1.3-2.0\,\mathrm{GeV}/c^2$. Nuclear effects for $\nu-{}^{16}\mathrm{O}$ scattering are also taken into account. Fermi motion of nucleons is simulated using the relativistic Fermi gas model. Pauli blocking effect is considered in the simulation of quasi-elastic scattering and single meson production. Pions generated in ${}^{16}\mathrm{O}$ are tracked taking into account their inelastic scattering, charge exchange and absorption. The pion generation point in the nucleus is set according to Woods and Saxon's nucleon density distribution [19]. The mean free path of each pion interaction is calculated using the model by Salcedo et al. [20]. The direction and momentum of pions after inelastic scattering or charge exchange are determined based on the results of a phase shift analysis obtained from $\pi-N$ scattering experiments [21]. Emission of de-excitation low energy γ-rays from a hole state of residual nuclei is also taken into account [22]. Outside the nucleus, particles are tracked using GEANT and CALOR packages except pions with momenta below $500\,\mathrm{MeV}/c$, which are tracked with a custom program [18] including the effect of the Δ resonance.

The NC1π^0 fraction in the single π^0 sample is estimated to be 71 % using the neutrino Monte Carlo simulation (52 % from single π^0 production via resonance decay, 3 % from single $\pi^\pm$ production via resonance decay and subsequent charge exchange into π^0 in the target nucleus, 10 % from coherent π^0 production and 4 % from neutrino deep inelastic scattering where the rest of the mesons are absorbed inside the nucleus). The non-NC1π^0 component accounts for 26 % of the single π^0 sample as shown in Figures 2 and 3. The non-NC1π^0 component contains NC π^0

Sources	Systematic Errors (%)
(A) Background Subtraction	
M_A in quasi-elastic and single meson ($\pm$10 %)	0.2
Quasi-elastic scattering (total cross section, $\pm$10 %)	0.0
Single meson production (total cross section, $\pm$10 %)	0.9
Coherent pion production (model dependence)	1.6
Deep inelastic scattering (model dependence)	5.1
Deep inelastic scattering (total cross section, $\pm$5 %)	0.5
CC/NC cross section ratio ($\pm$20 %)	3.2
Nuclear effects in ^{16}O (pion absorption, $\pm$30 %)	1.5
Nuclear effects in ^{16}O (pion inelastic scattering, $\pm$30 %)	0.7
Pion interaction outside the target nucleus ($\pm$20 %)	2.3
(B) Fiducial Volume Correction	
Fiducial cut	1.6
(C) Efficiency Correction	
Ring counting	5.4
Particle identification	4.2
Energy scale	0.3

Table 2
Summary of the systematic errors on the measurement of the number of NC1π^0 interactions.

production where outgoing mesons except a single π^0 have low momenta (7 %), CC π^0 production where accompanying muon and mesons have low momenta (9 %), and π^0 production by a recoil nucleon or mesons outside the target nucleus (10 %). The non-π^0 component caused by mis-reconstruction accounts for the remaining 3 % of the single π^0 sample.

The NC1π^0 fraction and the background fraction are estimated for each of the nine π^0 momentum bins shown in Figure 3. The number of NC1π^0 events is extracted from the number of observed single π^0 events multiplied by the NC1π^0 fraction bin by bin. The systematic errors of this background subtraction are estimated based on the uncertainties of neutrino interactions as listed in Table 2 -(A). The error due to the uncertainty on the deep inelastic scattering cross section is evaluated by comparing the two models in Refs. [15] and [16]. For coherent pion production, the difference between the two models in Refs. [13] and [14] is assumed to be the uncertainty. The systematic error in the CC component subtraction is estimated by considering the uncertainty on the CC cross section relative to the NC cross

section [23]. The systematic errors due to uncertainties on pion nuclear effects in the target nucleus are evaluated by varying the probabilities of pion absorption and inelastic scattering (including charge exchange) in the ^{16}O nucleus independently by $\pm 30\,\%$ [9]. The uncertainty on the cross section of $\pi - ^{16}$O interactions outside the target nucleus is taken from Refs. [24] and [25].

For the number of NC1π^0 events, we apply a 2 % fiducial correction, estimated using the Monte Carlo simulation, to account for the difference between the number of events in the true 25 ton fiducial volume and the number in the reconstructed fiducial volume. The vertex distribution of the π^0 events is in good agreement with that of the Monte Carlo events. The systematic error due to the uncertainty of the fiducial volume is estimated to be 1.6 % as shown in Table 2 -(B) by varying the boundary of the fiducial volume by ± 30 cm along the beam direction, which is the vertex resolution of the π^0 events.

Finally, the number of NC1π^0 interactions in the true 25 ton fiducial volume is corrected for the detection efficiency bin by bin. Figure 3 -(b) shows the detection efficiency for NC1π^0 interactions as a function of real π^0 momentum. The inefficiency for higher momentum π^0s results from the reconstruction of only one ring of a π^0 decay with highly asymmetric energies or a small opening angle between the two γ-rays. The overall detection efficiency for NC1π^0 interactions, estimated by the Monte Carlo simulation, is 47 % as shown in Table 1. The systematic errors from the efficiency correction are due to uncertainties of reconstruction algorithms such as ring counting, particle identification and energy scale as listed in Table 2 -(C).

After corrections for background subtraction, the true/reconstruction fiducial difference and the detection efficiency, the true number of NC1π^0 interactions is measured to be $(3.61 \pm 0.07 \pm 0.36) \times 10^3$ in the 25 ton fiducial volume. Figure 4 shows the measured momentum distribution of NC1π^0 after all corrections, compared with the distribution predicted by the neutrino Monte Carlo simulation. The Monte Carlo histogram is normalized by the total number of neutrino events in the fiducial volume after all the cuts. The size of inner boxes for the Monte Carlo histogram represents the statistical errors of Monte Carlo events. There exists small discrepancy between the measured distribution and the Monte Carlo expectation in the π^0 momentum around 300 MeV/c and 600 MeV/c. The size of outer boxes includes the error in the shape of the π^0 momentum distribution due to the uncertainties of nuclear effects, where the largest source is inelastic scattering of pions in the target ^{16}O nucleus. Considering these uncertainties, the discrepancy in the momentum distribution can be explained. The effect from this discrepancy is not significant in the cross section measurement.

As previously described, we use CC interactions for normalization in order to derive the relative cross section for NC1π^0 interactions. To make a CC enriched sam-

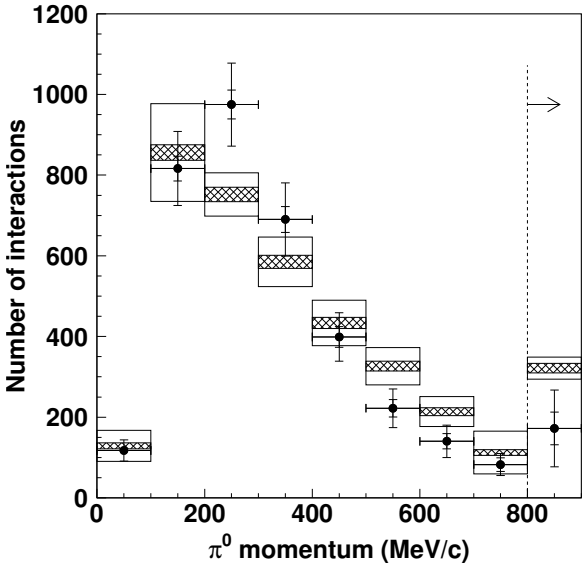

Fig. 4. The momentum distribution of NC1π^0 events in the 25 ton fiducial volume (black dots). The inner and outer error bars attached to data points show statistical errors and total errors including systematic errors, respectively. The distribution predicted by the neutrino Monte Carlo simulation is also shown as a box histogram for comparison. The size of inner boxes represents the statistical errors. The size of outer boxes includes uncertainties on nuclear effects of pions in ^{16}O.

ple, FC μ-like events and PC events are selected in the same period. By using the CC enriched sample as a normalization, the uncertainty of the neutrino energy spectrum [5] is almost canceled in the measurement since the expected mean energy of neutrinos producing the CC sample, 1.45 GeV, is almost same as that of neutrinos producing the π^0 sample, 1.50 GeV. The sample consists of 22,612 FC single-ring μ-like events, 12,386 FC multi-ring events with the most energetic ring identified as μ-like and 15,228 PC events, resulting in a total of 50,226 events. The ν_μCC fraction in this sample is estimated to be 96 % by the Monte Carlo simulation (96.5 % for the FC single-ring μ-like sample, 91.2 % for the FC multi-ring μ-like sample and 98.5 % for the PC sample). The remaining 4 % of the sample is mostly composed of NC interactions with an outgoing charged pion above its Cherenkov threshold. The fiducial volume correction factor is estimated to be 1.02. The detection efficiency for ν_μCC interactions by this selection is estimated to be 85%. The inefficiency mainly comes from mis-identification of the ring type in multi-ring events and $\sim$ 100 MeV visible energy threshold by peak counting of the PMTSUM signal.

By applying non-ν_μCC background subtraction, fiducial volume correction and detection efficiency correction, the number of ν_μCC neutrino interactions during the analysis period is measured to be $(5.65 \pm 0.03 \pm 0.26) \times 10^4$ in the 25 ton fiducial volume. The systematic errors are estimated to be 4 % from the uncertainty of vertex reconstruction, 1 % from the uncertainty of neutrino interaction models, 1 % from the uncertainty of particle identification and 1 % from the uncertainty of

absolute energy scale.

By taking the ratio, the relative cross section for NC1π^0 interactions to the total ν_μCC cross section is measured to be $0.064 \pm 0.001\,(stat.) \pm 0.007\,(sys.)$. Since the systematic errors on the NC1π^0 measurement and the ν_μCC measurement have almost no correlation, errors are added in quadrature. Our neutrino interaction model predicts the ratio to be 0.065, which is in good agreement. For reference, the total ν_μCC cross section is calculated to be 1.1×10^{-38} cm^2/nucleon in the neutrino Monte Carlo simulation averaged over the K2K neutrino beam energy.

In summary, we have measured the cross section and the π^0 momentum distribution of NC single π^0 production for neutrinos with a mean energy of 1.3 GeV using the K2K 1kt water Cherenkov detector. The ratio of cross sections for NC1π^0 to the total ν_μCC interaction is measured to be $0.064 \pm 0.001\,(stat.) \pm 0.007\,(sys.)$, showing good agreement with the prediction by our neutrino interaction model. This measurement provides essential information to understand π^0 production in water in the 1 GeV neutrino energy region, and is relevant to present and future neutrino oscillation experiments.

Acknowledgements

We thank the KEK and ICRR Directorates for their strong support and encouragement. K2K is made possible by the inventiveness and the diligent efforts of the KEK-PS machine and beam channel groups. We gratefully acknowledge the cooperation of the Kamioka Mining and Smelting Company. This work has been supported by the Ministry of Education, Culture, Sports, Science and Technology, Government of Japan and its grants for Scientific Research, the Japan Society for Promotion of Science, the U.S. Department of Energy, the Korea Research Foundation, the Korea Science and Engineering Foundation, the CHEP in Korea, and Polish KBN grant 1P03B03826 and 1P03B08227.

References

[1] Y. Fukuda, et al., Phys. Rev. Lett. 81 (1998) 1562.

[2] M. H. Ahn, et al., Phys. Rev. Lett. 93 (2004) 051801.

[3] S. H. Ahn, et al., Phys. Lett. B511 (2001) 178.

[4] Y. Itow, et al., hep-ex/0106019.
URL `http://neutrino.kek.jp/jhfnu/`

[5] M. H. Ahn, et al., Phys. Rev. Lett. 90 (2003) 041801.

[6] Y. Fukuda, et al., Nucl. Instrum. Meth. A501 (2003) 418.

[7] Y. Fukuda, et al., Phys. Lett. B433 (1998) 9.

[8] M. Shiozawa, Nucl. Instrum. Meth. A433 (1999) 240.

[9] Y. Hayato, Nucl. Phys. Proc. Suppl. 112 (2002) 171.

[10] C. H. Llewellyn Smith, Phys. Rept. 3 (1972) 261.

[11] D. Rein, L. M. Sehgal, Ann. Phys. 133 (1981) 79.

[12] S. K. Singh, M. J. Vicente-Vacas, E. Oset, Phys. Lett. B416 (1998) 23.

[13] D. Rein, L. M. Sehgal, Nucl. Phys. B223 (1983) 29.

[14] J. Marteau, J. Delorme, M. Ericson, Nucl. Instrum. Meth. A451 (2000) 76.

[15] M. Gluck, E. Reya, A. Vogt, Z. Phys. C67 (1995) 433.

[16] A. Bodek, U. K. Yang, Nucl. Phys. Proc. Suppl. 112 (2002) 70.

[17] T. Sjostrand, Comput. Phys. Commun. 82 (1994) 74.

[18] M. Nakahata, et al., J. Phys. Soc. Jap. 55 (1986) 3786.

[19] R. D. Woods, D. S. Saxon, Phys. Rev. 95 (1954) 577.

[20] L. L. Salcedo, E. Oset, M. J. Vicente-Vacas, C. Garcia-Recio, Nucl. Phys. A484 (1988) 557.

[21] G. Rowe, M. Salomon, R. H. Landau, Phys. Rev. C18 (1978) 584.

[22] H. Ejiri, Phys. Rev. C48 (1993) 1442.

[23] E. H. Monsay, Phys. Rev. Lett. 41 (1978) 728.

[24] J. P. Albanese, et al., Nucl. Phys. A350 (1980) 301.

[25] A. S. Clough, et al., Nucl. Phys. B76 (1974) 15.